Coarse-grained Simulation of Anionic Surfactant Sodium Dodecyl Sulfate

Xiang-feng Jia (Jiaxf@sdjzu.edu.cn)
School of Municipal and Environmental Engineering, Shandong Jianzhu University, Jinan, 250100 China

Jing-fei Chen
Shandong Provincial Key Laboratory of Synthetic Biology, Qingdao Institute of Bioenergy and Bioprocess Technology, Chinese Academy of Sciences, Qingdao

Hui-xue Ren
School of Municipal and Environmental Engineering, Shandong Jianzhu University, Jinan

Qi Wang
School of Municipal and Environmental Engineering, Shandong Jianzhu University, Jinan

Wen Xu
School of Municipal and Environmental Engineering, Shandong Jianzhu University, Jinan

Yong-shan Ma
School of Municipal and Environmental Engineering, Shandong Jianzhu University, Jinan

Xue-mei Li
School of Municipal and Environmental Engineering, Shandong Jianzhu University, Jinan

Research Article

Keywords: Catanionic surfactant, Molecular dynamical simulation, Vesicle, Self-assembly, Coarse grained method

Posted Date: January 4th, 2021

DOI: https://doi.org/10.21203/rs.3.rs-136348/v1

Coarse-grained Simulation of Anionic Surfactant Sodium Dodecyl Sulfate

Xiang-feng Jia[1,*], Jing-fei Chen[2,+], Hui-xue Ren[1], Qi Wang[1], Wen Xu[1], Yong-shan Ma[1], Xue-mei Li[1]

[1]School of Municipal and Environmental Engineering, Shandong Jianzhu University, Jinan, 250100 China

[2]Shandong Provincial Key Laboratory of Synthetic Biology, Qingdao Institute of Bioenergy and Bioprocess Technology, Chinese Academy of Sciences, Qingdao, 266101, China

[*]Xiang-feng Jia Jiaxf@sdjzu.edu.cn

[+]Jingfei Chen contributed equally to this work

Abstract

Through analyzing the deficiency of the current coarse-grained (CG) model, a new CG model for the ionic surfactant was proposed based on the Martini force field and iterative Boltzmann inversion method. In this model, the electrostatic interaction can be tackled by using a self-defined piecewise function to avoid the disadvantage of using coarse-grained solvents, and the VDW interaction parameters were derived by iterative methods. Using the improved model, the radial distribution function of NaCl and SDS solution in all-atom OPLS can be completely reproduced. The successful setup of the new coarse-grained model provides a good example of the construction of a high-precision coarse-grained force field.

Keywords: Catanionic surfactant, Molecular dynamical simulation, Vesicle, Self-assembly, Coarse grained method

1. Introduction

Molecular dynamics simulation is a powerful approach to studying the properties of lipid aggregates, self-assembly on a gas-liquid interface, surfactant interaction with new carbon materials and the interaction between surfactants and polymers.[1,2] However, many processes that occur in liquids, soft materials and biomolecular systems occur over length and time scales that are well beyond the current capabilities of atomic-level simulation, such as using molecular dynamics model (all-atom, AA and united-atom, UA). As such, new and novel approaches continue to be developed that can access longer time and length scale phenomena. One such approach is coarse-grained (CG) simulation.[3] The post representative CG method is the Martini force field developed by the group of Marrink and Tieleman for many different lipids,[4-7] protein,[8-10] polymers[11-13] and sugar[14-15] and other more.[16-18] The Martini model is based on a four-to-one mapping, i.e. on average four heavy atoms plus associated hydrogens are represented by a single interaction center. This model aims for a broader range of applications without the need to reparameterize the model each time. A top-down approach is used by the extensive calibration of the nonbonded interactions of the chemical building blocks against experimental data, in particular, thermodynamic data such as oil/water partitioning coefficients. And this greatly improves the universality of the force field. Currently, the Martini force field is ideally suited to study the formation of micelles in solutions.[19-25] In a study comparing some surfactants, the Martini model reproduced experimental Critical micelle concentrations (CMCs) and aggregation numbers for non-ionic surfactants reasonably well.[26-27] Also, the group of Klein (W. Shinoda, R. Devane, and M. L Klein) established the new coarse-grained intermolecular force field (in short SDK) for a series of zwitterionic lipids. The model is designed to reproduce experimental

surface/interfacial properties using simple function forms. Although there are many topologies of phospholipid molecules and surfactant molecules in the existing Martini force field and SDK force field,[28-29] they are not universality for the traditional typical surfactant systems, especially the ionic surfactant systems. For example, the Martini force field belongs to the semi-quantitative coarse-grained field, it is necessary to reiterate the parameters repeatedly to obtain a more reasonable simulation value. The process is more complicated.

In this paper, we will use take the most common anionic surfactant SDS (sodium dodecyl sulfate) as an example, based on the Martini force field to improve and establish a coarse-grained force field with higher accuracy. The effectiveness of the force field is tested by reproducing the basic physicochemical properties of SDS in the aqueous solution. It is expected that a set of coarsening force fields belonging to the surfactant system will be modified according to this method.

Results

LJ Potential Energy Function and Radial Distribution Function in Single-Component Van Der Waals Particle System

In the single-component Van der Waals particle systems, we used the Martini coarse-grained force field to perform molecular dynamics simulations on three simple particle systems, to analyze the relationship between the LJ potential energy function and the radial distribution function. The simulation was conducted with a pressure P of 1 bar and a temperature of 303K, and the particle mass (m) was set to 72 with the number of 400. The simulation time was 2 ns, and the constant σ was set 0.47 nm and ε were set 0.1 KJ/mol, 2 KJ/mol, and 4 KJ/mol, respectively. All the simulations were performed

with Gromacs 5.0[30] package. It can be seen from Figure.1 that the radial distribution function among the particles is single-peak in all systems because there are only one species of the particle in them. The height of the peak gradually decreases and the shape of the peak also changes from a sharp peak to a broad peak, when the interaction strength between the particles decreases. It should be noted that no matter how the intensity of the peak changes, the left side of the single peak always changes around the σ value (0.47nm). Specifically, the highest of the peak is closer the σ value when the intensity of the peak is low, whereas it is farther to the σ value. Therefore, we can adjust continuously the σ value and ε value between particles in the coarse-grained system, based on the radial distribution function between CG units in all-atom or united-atom force field simulation results. Finally, the fitting CG force field can be obtained in the single-component system.

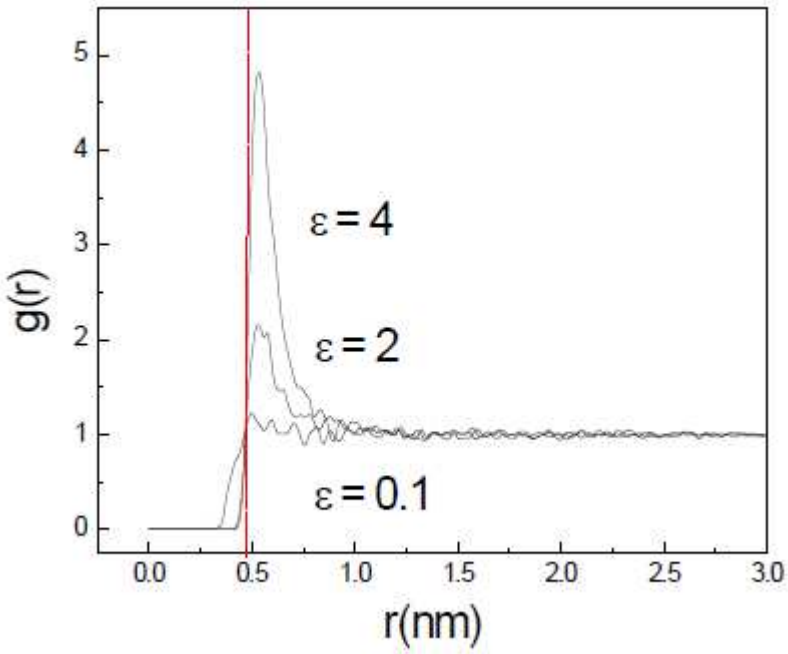

Figure 1. In the single-component Van der Waals systems, the radial distribution function (RDF) of the particles with the same σ_{ij} (0.47nm) but different ε_{ij} (0.1, 2, 4 KJ/mol). The σ value are indicated by the dash line.

LJ Potential Energy Function and Radial Distribution Function in Two-Component Van Der Waals Particle System

In the experiment, the single-component system was too simple and more multi-component systems were used. Next, the relationship between the radial distribution function and potential energy function will be analyzed in the van der Waals system containing two kinds of particles. Assume that there are solute particles (S) and solvent particles (W) in the system, and the interaction parameters of solvent molecules are $\sigma_{ww=0.47nm}$ and ε_{ww}=5kJ/mol (which are the coarse grain model of water in the Martini force field). Both σ_{ss} and σ_{sw} are also set to 0.47nm, respectively. By changing the values of ε_{ss} and ε_{sw} continuously to simulate the variation of the radial distribution function solutes with different polarities and solubilities in the same solvent. In the simulation process, the number of solute S and solvent W in the simulation box was set to 50 and

400, respectively, and other conditions were consistent with the simulation conditions in the single-component system.

It can be seen from Figure 2. that the radial distribution function between the solute particles S becomes complicated due to the addition of the solvent particles W. This is the fact that the solute particles S are surrounded by the solvent particles W, and the energy barrier caused by the solvent particles W needs to be overcome when the solute particles S come close to each other. However, no matter how the polarity (ε_{ss}) and the solubility (ε_{sw}) of the solute molecules change, the left side of the main peak in the RDF curve always changes around σ_{ss}, and shows the same change rule as the position of the main peak of the single-component system. In the strongly polar and strongly soluble system(Figure 2a.), there are more peaks in the RDF curve and the troughs between the peaks are deeper. The height of the main peak on the RDF curve rapidly increases (from 2.5 to 17) and the latter peak becomes weaker than the main peak, if the polarity of the solute remains unchanged and the solubility becomes small (Figure 2b.). When both polarity and solubility are reduced (Figure 2c.), the height of the main peak does not change much and the latter peak is slightly weaker compared with the curve in Figure 2a. As generally seen in Figure 2a. and Figure 2c., the change of peaks is not obvious in appearance. It is worth noting that the main peak of RDF will be lower than the height of the latter peak, in the low polarity and high solubility system (seen in Figure 2d.).

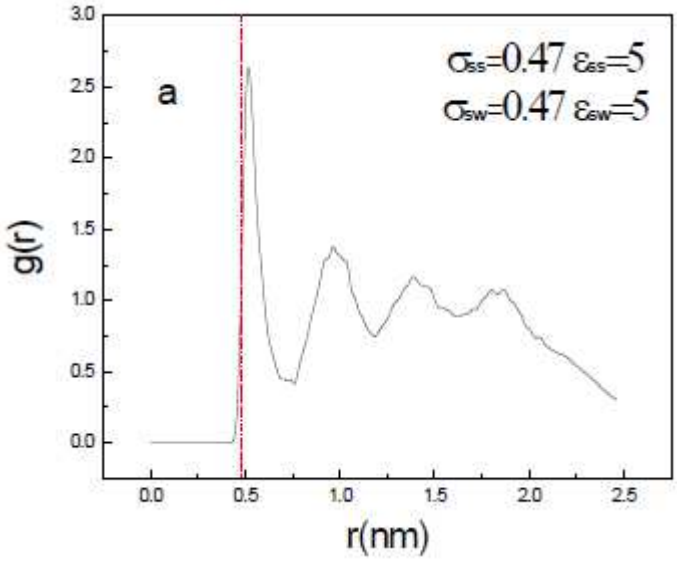
a
σss=0.47 εss=5
σsw=0.47 εsw=5
g(r)
r(nm)
0.0
0.5
1.0
1.5
2.0
2.5
3.0

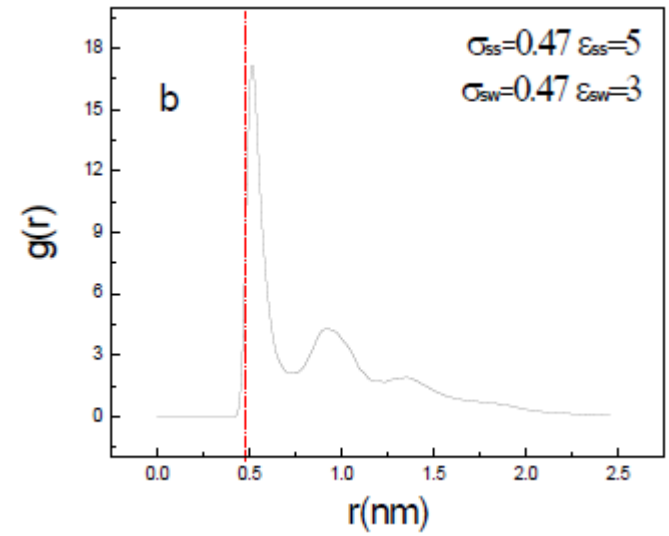
b
σss=0.47 εss=5
σsw=0.47 εsw=3
g(r)
r(nm)
0
3
6
9
12
15
18
0.0
0.5
1.0
1.5
2.0
2.5

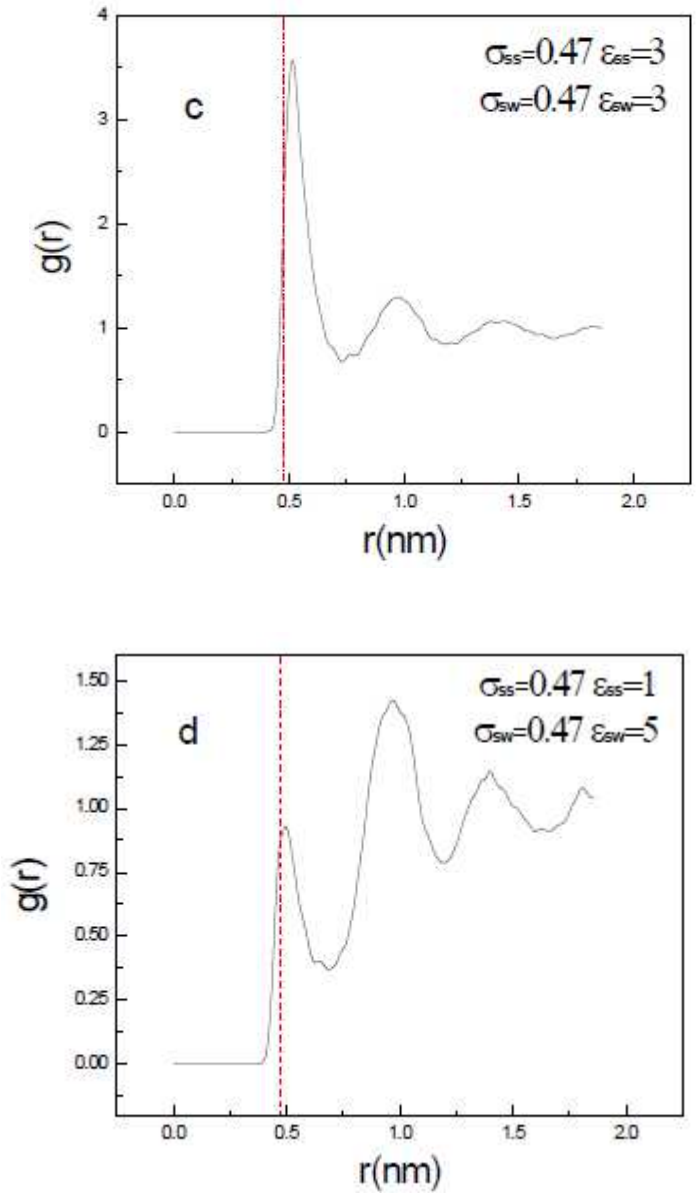

Figure 2. RDF of particles with different polarity and solubility in the same solvent, $g_{s\text{-}s}(r)$. σ_{ss}(0.47nm) are indicated by dash lines.

In summary, the RDF curve between solute molecules has the following rules: The main peak height is determined by the polarity and solubility of solute molecules. The solute with strong polarity (large ε_{ss} value) and low solubility (small ε_{sw}) has the highest peak value. While the intensity of small peaks relative to the main peak is mainly

determined by the solubility, larger solubility results in smaller peaks. On the contrary, it is weak. Although the above rules are all derived with the same conditions of σ, when σ changes, the above rules are suitable even if the complexity of the peaks increases.

Radial Distribution Function of Charged Particles in Aqueous Solution

There is electrostatic force expect Van der Walls forces in the solution of charged particles. Using sodium chloride as an example, we first study the characteristics of the radial distribution function in a solution of a simple charge particle by the optimized potentials for liquid simulation all-atom (OPLS-AA) force field. The action parameters of chloride ion and sodium ion can be seen in Table 1. The water molecules is represented by SPC/E[31] (extended simple point charge) water model.

The simulation conditions were set as follows: The number of sodium ions, bromide ions and water molecules were 50, 50 and 2000, respectively. The simulation step was 5fs and the simulation time was 5ns. The temperature and pressure were the same as those of the previous two systems.

Table 1. The σ and ε values of Na^+ and Cl^- inOPLS-AA force field[32,33]

particle	σ(nm)	ε(kJ/mol)
Na^+	0.3330	0.0116
Cl^-	0.4417	0.4928

Addition Na^+ and Cl^- in aqueous systems, Figure 3. shows that the relationship between the main peak of the RDF and the σ value no longer follows the rules of the first two systems. This is due to the fact that the electrostatic attraction between Na^+ and Cl^- particles is much greater than the Van der Waals forces. So it appears on RDF curve that

the equilibrium distance between Na^+ and Cl^- is much smaller than the σ value between them. Due to the large repulsive force between Na^+ and Na^+, Cl^- and Cl^-, the intensity of the peaks on the RDF curve is very small, which is almost close to 1. Next, we only focus on the RDF between Na^+ an Cl^- appearance.

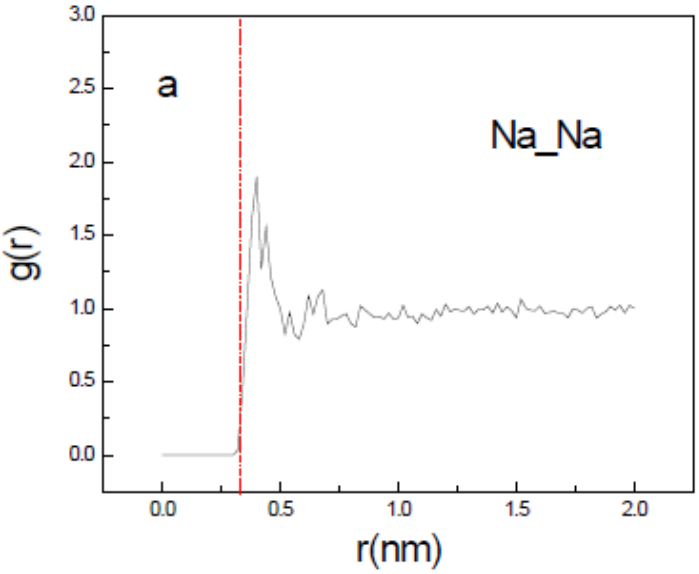

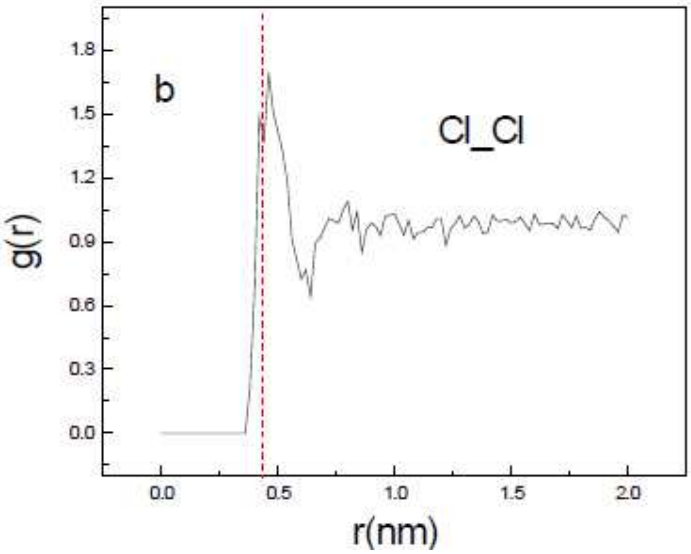

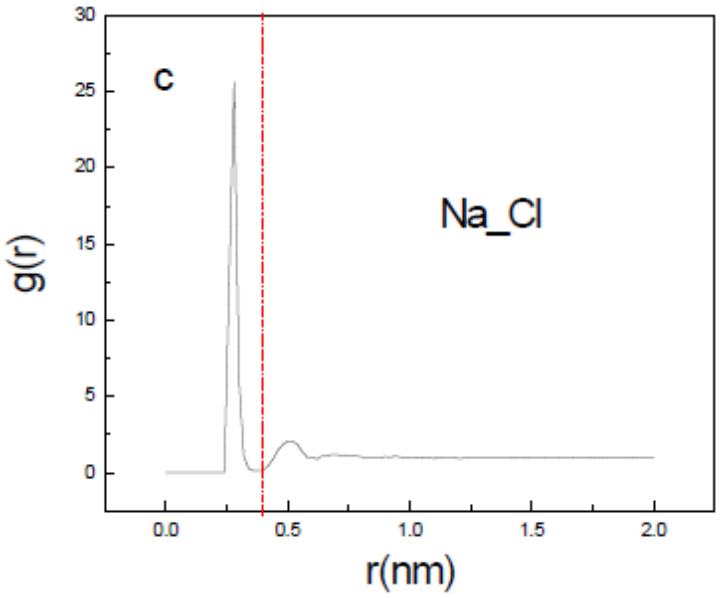

Figure 3. RDF

between the charged particles in the NaCl solution, the σ values between the particles was indicated by dash lines.

There are two peaks in Figure 3c. The first peak is very high and located exactly to the left of σ_{NaCl}, while the second is much weaker. This shows the electrostatic effect between Na^+ and Cl^- is the strongest, when the distance between them is less than the minimum distance of Van der Waals action. However, when this distance is exceeded, the electrostatic interaction between Na^+ and Cl^- rapidly decreases due to the hydration effect. What is worth noting is how the second small peak is formed? From the perspective of location, it is not formed through Van der Waals action. Figure 4. vividly illustrates the reasons.

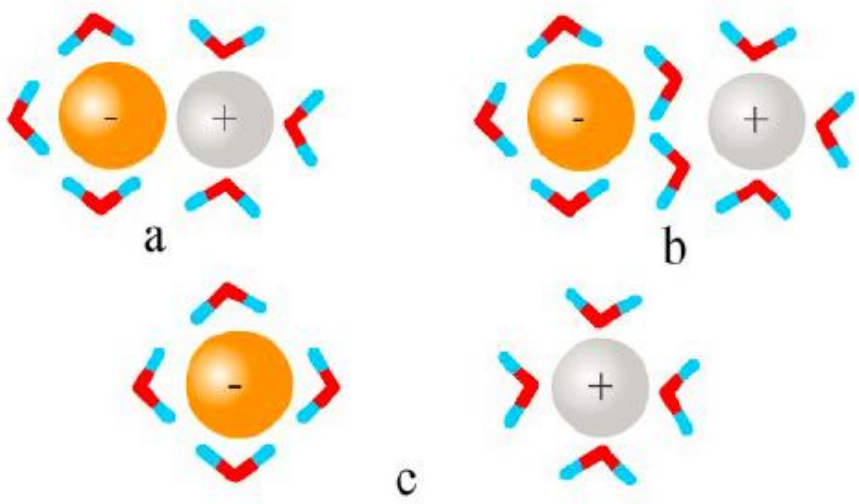

Figure 4. Different hydration states of Na^+ and Cl^- in NaCl solution

Figure 4a shows that there is a strong electrostatic attraction between the anions and cations, when the distance between anions and cations is less than the minimum distance of Van der Waals action. As the distance between them increase, hydration increases and electrostatic attraction decreases. When in state Figure 4b., although the water molecules located between the anions and cations also play a role in hydration, the water molecular at this time mainly play the role of "bridge". That is one end of the water molecule with a positive charge faces the anion, and the other end with a negative charge faces the cation. At this moment, the anions and cations in this state are also relatively stable, and this state corresponds exactly to the second peak in Figure 3c. So when the distance between Na^+ and Cl^- continues to increase in NaCl aqueous, both Na^+ and Cl^- are in a fully hydrated state, the electrostatic force between them is relatively weak.

Discussion

The Coarse-grained simulation of aqueous NaCl solution

In the previous coarse-grained model, simple ions (such as Na^+, Cl^-,etc.) are often coarse-grained into one particle along with the hydrated water molecules. In the simulation process, the water molecules considered as the largest consumption of

calculated resources, coarsely granulates multiple water molecules into one particle through the “four-in-one” or “three-in-one” rule. Because the coarse-grained water molecules have no polarity, they can not effectively shield the charge of charged particles like the water molecules in AA or UA force field. In these coarse-grained force fields, therefore, the relative permittivity is modified to weaken the electrostatic force between the charged particles. By analyzing the hydration state of Na^+ and Cl^- in water, it can be concluded that the relative permittivity of aqueous solution will change with the distance between ions, which can be expressed by a piecewise function:

$$\begin{aligned} \varepsilon_r &= e^{10.89r} && r \le r_0 \\ \varepsilon_r &= 78 && r > r_0 \end{aligned} \tag{1}$$

In the above equation, r_0 represents the radius of hydration of the ions. When the distance r between ions is smaller than r_0, the relative permittivity ε_r can be expressed as an exponential function. when r is greater than r_0, ε_r is expressed as a constant 78 (the exponential function of water). Since most of ions have a hydration radius of 0.3-0.4nm, the r value is uniformly taken as 0.4nm in our model.

Table 2 lists the parameter in our coarse-grained force field. The non-bond parameters σ and ε of Na^+ and Cl^- also come from the OPLS field. The model of water directly uses the “four-in-one” coarse-grained model in the Martini force field. Therefore, it is only necessary to adjust the interaction about $Na^+(Cl^-)$ with W (the water’s CG particle), respectively. It is worth noting that we use the LJ(12-3) function, but not LJ(12-6) function, about the non-bonding interaction between $Na^+(Cl^-)$ and water coarse-grained particles W. This is because electrostatic interactions exist between charged ions and water molecules, and the LJ(12-3) function can more accurately reflect the interaction between the two.

Table 2 Coarse-grained force field for NaCl aqueous solution

particles		σ(nm)	ε(KJ/mol)
Na^+	W	0.4	1.5
Cl^-	W	0.4	1.0
W	W	0.47	5.0

It can be seen from Figure 5., our simulation results can reproduce RDF curve obtained using the OPLS force field. In Figure 5c, it should be pointed out that the second peak of the RDF curve can not be reproduced using the coarse-grained force field. It is due to the absence of the polarity in the coarse-grained water molecule model and the inability to truly reflect the hydration conditions about anions and cations.

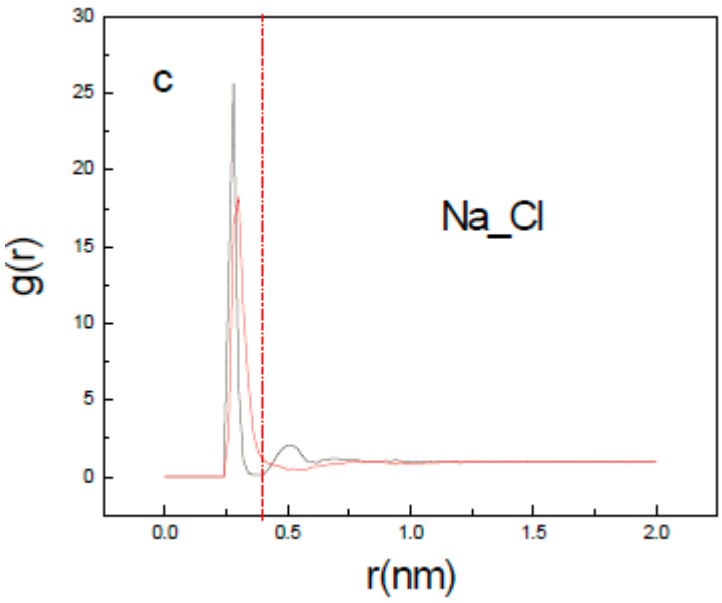

Figure 5. The RDF of ions in NaCl coarse grained system

Despitethis, our coarse-grained model can reproduce the NaCl aqueous sc

these subtle difference can be negligible, see Figure 6.

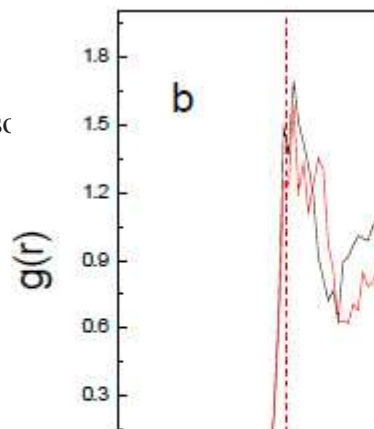

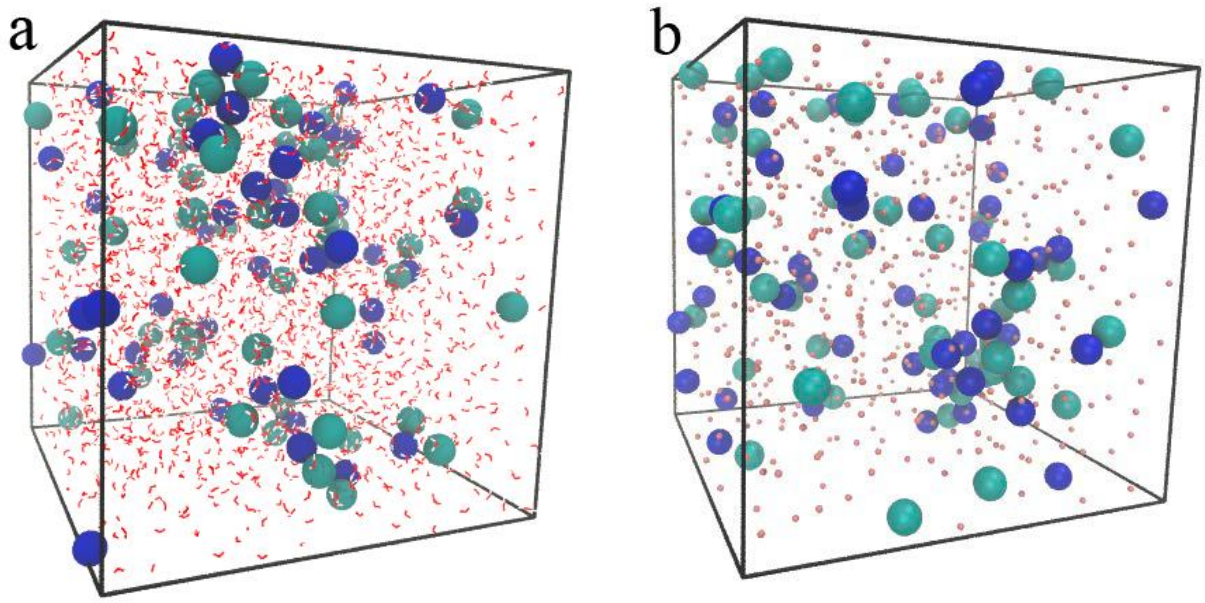

Figure 6. NaCl solution was simulated using OPLS-aa (a) and CG (b) force filed

The Coarse-grained of Sodium Dodecyl Sulfate Aqueous Solution

A set of simple rules can be summarized to adjust the interaction parameters of each coarse-grained particle, by analyzing the interaction between the RDF of particles in simple particle system and LJ potential energy and electrostatic potential energy. The most common anionic surfactant, sodium dodecyl sulfate (SDS), is used as an example to illustrate the adjustment process of parameters of the coarse-grained field of ionic surfactant.

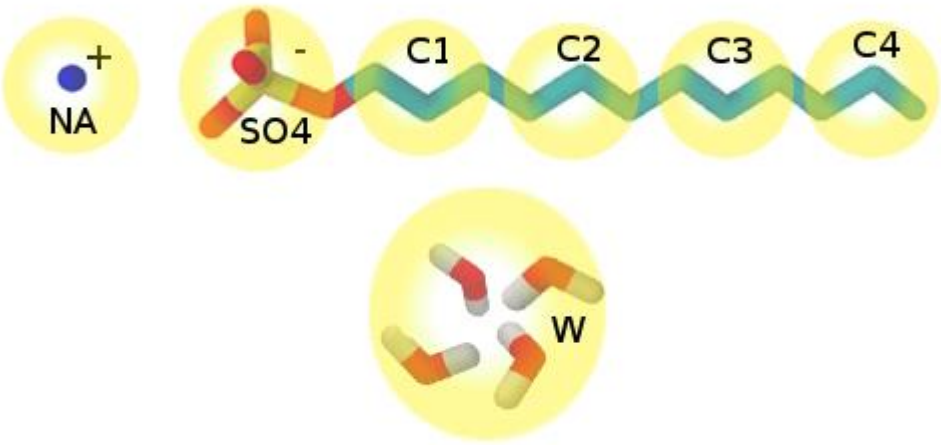

Figure 7. Coarse grained model of SDS

First, the SDS molecular model is divided into different coarse-grained cells, as shown in Figure 8. The head of the SDS molecule consists of one S atom and four O atom, and they are divided into a coarse-grained particle with a unit of negative charge(SO4 shown in Figure 7.). For the carbon atoms in the hydrophobic chain, the principle of "three-in-one" is adopted. That is three carbon atoms together with hydrogen atoms are used as a coarse-grained unit, and the hydrophobic tail is divided into four coarse-grained particles(C1, C2, C3and C4 shown in Figure 7.). The four CG particles are classified into two types. The CG particle of carbon attached to the head group(C1) are CE type ,the other three CG particle(C2, C3 and C4) are CT types. In other CG models, inorganic salt ions (such as Na^+ and Cl^- etc), together with hydrated water molecules, are often used as a CG unit. In our CG model, Na^+ is seen as an independent CG particle(NA shown in Figure 8.) with a positive unit charge. The advantage of this is that the simulation results can truly reflect the role Na^+ in the self-assembly of SDS molecules and increase the accuracy of the simulation.

The Bonded parameters in SDS Coarse-grained Model

In the SDS molecule, the potential energy between CG particles is in the form of a harmonic potential function：

$$E_{\text{bond}}(\text{r}) = \frac{1}{2} K_{\text{bond}} (r\text{-}r_0)^2 \tag{2}$$

$$E_{angle}(\theta) = \frac{1}{2} K_{angle} \{\cos(\theta) - \cos(\theta_0)\}^2 \tag{3}$$

Equation (2) and (3) represent the stretching vibration potential energy and the bond angle bending vibration potential energy in the CG particles. Where K_{bond} and K_{angle} represent the force constants of the stretching vibration and the bond angle bending vibration, and r_{bond} and θ_0 represent the equilibrium bond length and the equilibrium bond angle, respectively. The above parameters can be obtained by comparing with the results of using a fine force field to simulate SDS molecule, see Table 3. From the parameters of the intramolecular action, it can be seen that both the stretching vibration and the bending vibration of the bond angle are much large than the standard Martini force field. This is because the chain length of surfactants is shorter than that of large biomolecules, and therefore their softness is much lower.

Table 3 Bonded parameters for SDS in CG force field

Bond	r_0(nm)	K_{bond}(KJ·mol^{-1}·nm^{-2})
SO4-C1	0.37	40000
C1-C2	0.38	50000
C2-C3	0.38	50000
C3-C4	0.38	50000
Angle	θ_0(deg)	K_{angle}(KJ·mol^{-1}·rad^{-2})
SO4-C1-C2	180	500
C1-C2-C3	170	3000

C2-C3-C4	180	3000

Non-Bonded Parameters in the SDS Coarse-grained model

In the first half, we have summarized the relationship between the potential energy function and the RDF in a system where only van der Waals forces exist and a charged particle system. On this basis, we will try to estimate the potential energy parameters based on the RDF of partiles in in the CG system containing chemical bonds, thus, complete the CG process of the complex system. Unlike simple particle systems, the existence of chemical bonds leads to a stronger correlation between particles, and the RDF between them is more complicated. The SDS aqueous solution system is used as an example to describe the process of obtaining the model parameter in the ionic surfactant CG force field.

First, we obtain the RDF curve of SDS molecules in aqueous solution using the fine force field (OPLS-UA force field). The steps are as follows: In a cubic box with side length of 5.5nm, 10 SDS molecules were randomly placed, and then 4502 water molecules were added. Since the force field of the SDS molecules has been reported many times, there is no further verification of the reliability of the of force field. The water molecules adopts the SPC/E model. The simulations were performed in the NpT ensemble as taken in previous paper[34,35], the T (temperature) was kept at 303K by applying a Berendsen thermostat with the time constant to 0.1ps, and the *P* (pressure) was held constant at 1 bar using a Parrinello-Rahman barostat,with the time constant to 0.5ps. After the above setting, the simulation step can be set to 5fs. The simulation was performed in the molecular dynamics package Gromacs 5.0 with a simulation time of 20 ns. The last 10 ns of the trajectory was used to analyze the RDF between CG cells, as shown in Figure 8.

In the CG simulation system, the number of molecules such as SDS and water, and the simulations conditions such as temperature and pressure were all set exactly the same as those in the above system. The treatment for Van der Walls forces is the shift method. The values of rvdw_switch and rvdw are set as 0.9nm and 1.2nm, respectively. The electrostatic force still use a segmented approach, as shown in equation (1).

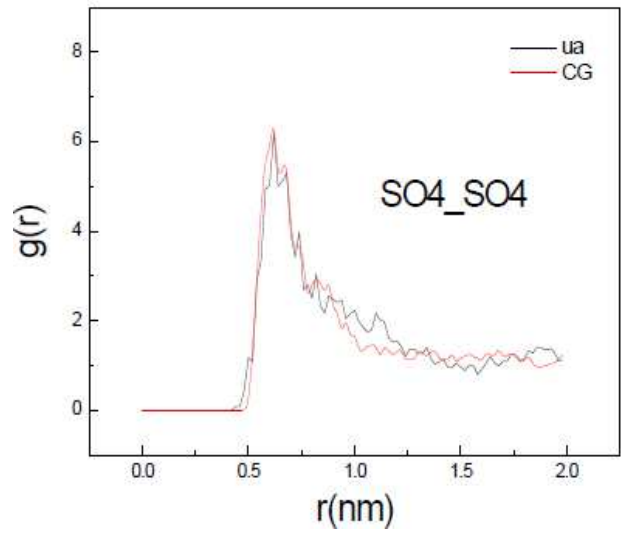
ua
CG
SO4_SO4
g(r)
r(nm)

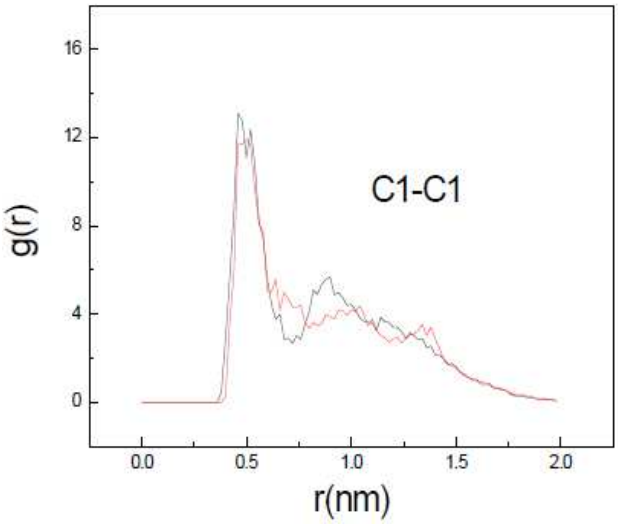
C1-C1
g(r)
r(nm)

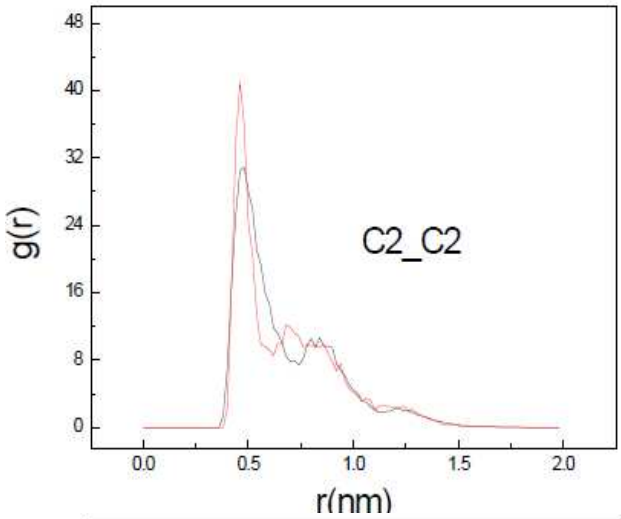
C2_C2
g(r)
r(nm)

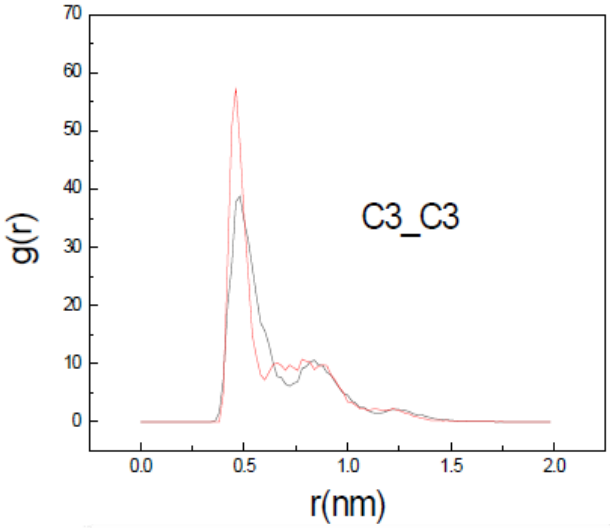
C3_C3
g(r)
r(nm)

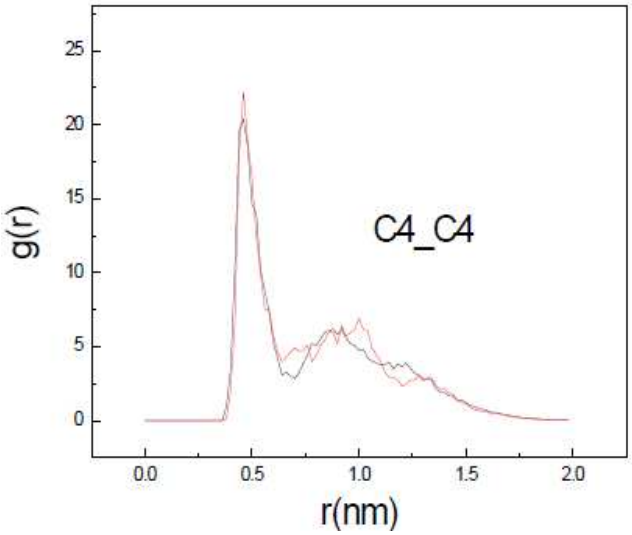
C4_C4
g(r)
r(nm)

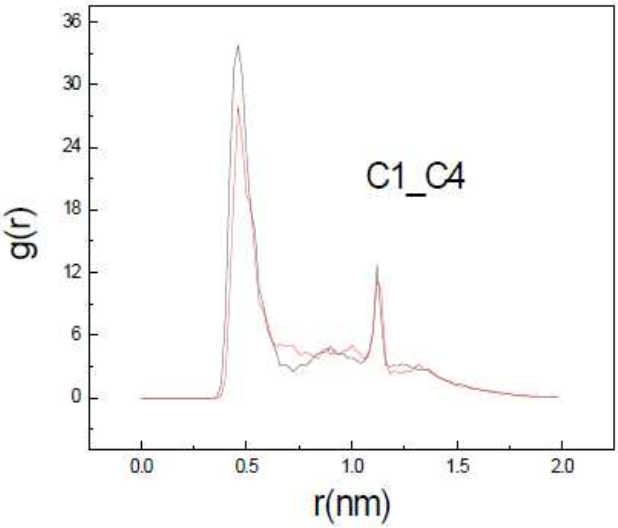
C1_C4
g(r)
r(nm)

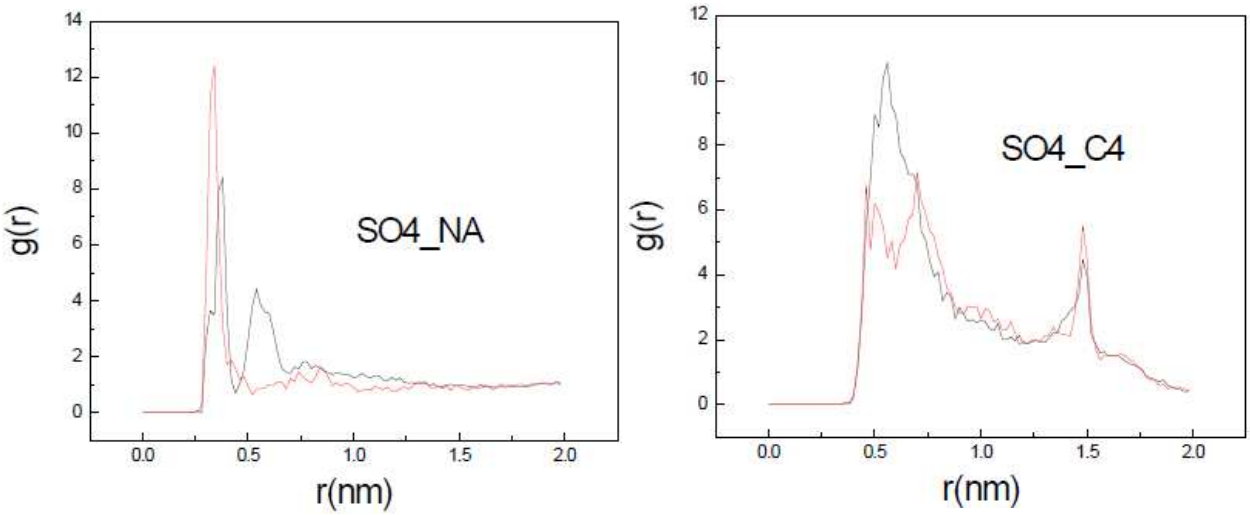

Figure 8. RDF of different units of SDS in unitedatomic (ua:—) and Coarse-grained (CG:—) simulation

Although the radius of SO4 is large than Na^+ or Cl^-, its hydration radius is not much different, so the parameters in the piecewise function of SO4 are exactly the same as those of Na^+ or Cl^-. Compared with the molecular model of the atomic level, the simulation step size can be modified to 20fs due to the greatly increased distance between CG units. In dealing with the intermolecular potential energy, we dealt with Van der Waals forces and electrostatic forces separately. Therefore, the RDF curves of CG system and the atomic (OPLS-UA force field) system can be realized the coincidence by repeatedly adjusting the Van der Walls potential energy parameters between the CG particles and comparing the RDF images of the CG system and the atomic system, the results shown in FIgure 8. Figure 9 shows the snapshots of SDS in atomistic (a) and the coarse grained (g) simulation, respectively. In essence, our CG method is consist with Boltzmann inverse iterative method.

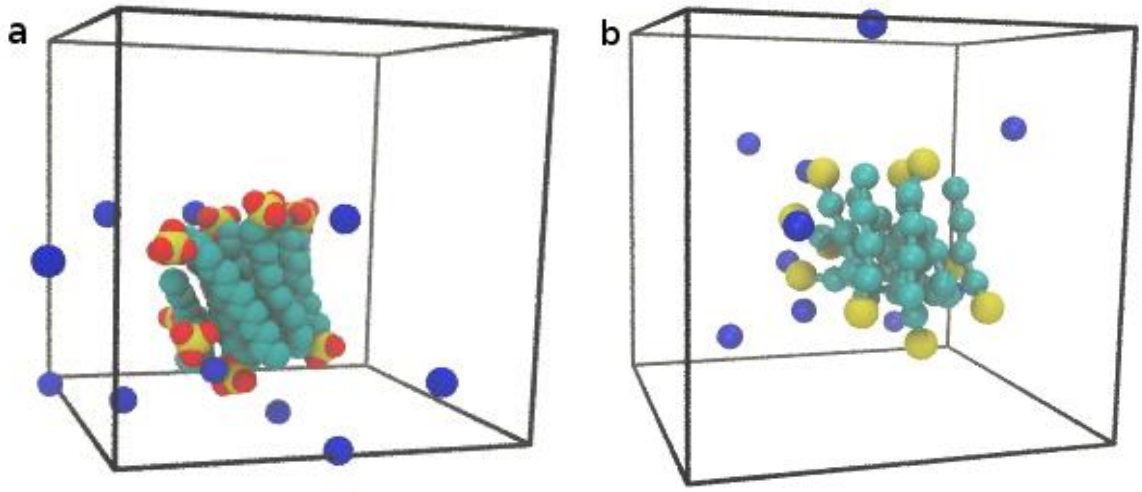

Figure 9. The snapshots of SDS micelles in atomistic (a) and coarse grained (b) simulation

In the process of adjusting coarse granulation parameters, the following matters should be paid more attention:

First, the σ value of the Van der Walls interaction between the CG units needs to be determined, because the σ value has the greatest influence on the RDF image between the two CG units. As mentioned earlier, the σ value between most CG particles is on the left side of the main RDF peak, except for the σ value between the CG particles with positive and negative charges. So the σ value can e directly estimated from the RDF curve.

The second, the intensity of CG RDF curve can generally be adjusted by the value of ε, the higher the peak intensity, the larger ε value.

The third, when fitting the potential energy parameters between charged CG units such as SO4-SO4, and SO4-NA, we must consider the adjustment of the RDF among other particles. This process is actually a matter of balancing electrostatic potential energy and Van der Waals potential energy. After adjusting, potential energy relationships between CG units in the SDS molecule can be obtained, as shown in Table 4.

Table 4. The LJ potential parameters in SDS CG simulation

i	j	σ_{ij}(nm)	ε_{ij}(KJ/mol)	
CE	CE	0.42	2.7	
CT	CT	0.42	2.7	
CE	CT	0.42	2.7	
SO4	SO4	0.53	3.0	Form OPLS force
NA	NA	0.33	0.01	field
SO4	CE	0.43	2.0	
SO4	CT	0.43	2.0	
SO4	NA	0.5	0.008	
NA	CE	0.5	1.2	
NA	CT	0.5	1.2	
W	NA	0.4	1.0	The σ value between each CG unit and W is specified as 0.4nm.
W	SO4	0.4	2.5	
W	C4	0.4	1.5	
W	C4	0.4	1.5	

Conclusion

In this article, we propose a new CG model for ionic surfactants by improving the electrostatic treatment and the fitting method of Van der Walls in the original CG model. The model can well reproduce the RDF curves of NaCl and SDS aqueous solution system. This initially realizes the establishment of a high-precision CG force field, and lays a good foundation to accurately simulate the large scale surfactants.

Methods

Like the traditional molecular force field, the common CG force field also uses the same potential energy expression form:

$$E_{mol} = E_{intra} + E_{inter} \quad (4)$$

That is, the energy of the entire molecular system (E_{mol}) is divided into the intramolecular potential energy(E_{intra}) and the intermolecular potential energy (E_{inter}). The parameters of E_{intra} can be obtained by comparing the corresponding CG units with the united-atom or the all-atom model, and repeatedly adjusting the stretching and the bending vibration constants in the CG model. The treatment of E_{inter} will directly affect the precision and universality of the CG force field, compared with E_{intra}. Therefore, the key task in developing the CG force field is to fit the non-bonded potential energy function. In terms of function, the E_{inter} also adopts the similar function form of traditional molecular dynamics, in which the E_{inter} consists of van der Waals potential energy and electrostatic potential energy (Equation 2)

$$E_{\text{inter}} = E_{vdw}(\text{r}) + E_{el}(\text{r}) \tag{5}$$

$$E_{vdw}(r) = 4\varepsilon_{\text{ij}}[(\frac{\sigma_{ij}}{r})^{12} - (\frac{\sigma_{ij}}{r})^{6}] \tag{6}$$

$$E_{el}(r) = \frac{q_i q_j}{4\pi_0 \pi_r r} \tag{7}$$

For the van der Waals forces between different coarse-grained units, the most commonly Lennard-Jones12-6[30] potential energy functions form was used (see in equation 6). Wherre σ_{ij} represents the minimum distance between interaction particles and ε_{ij} represents the strength of the interaction between them as shown in Figure 10.

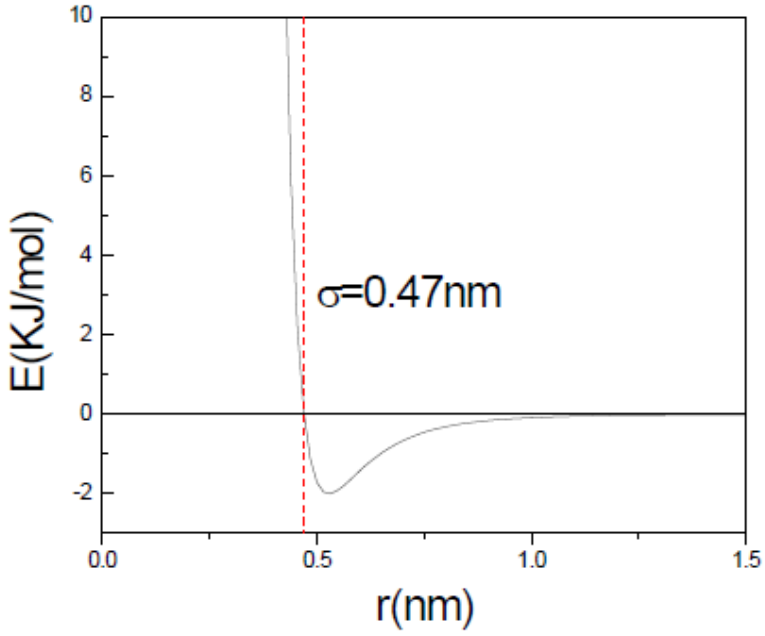

Figure 10. Lennard-Jones interaction (12-6)

References:

1. Marrink,S.J. De,Vries, A.H. Tieleman, D.P. Lipids on the move: Simulations of membrane pores, domains, stalks and curves. *BBA-Biomembr.* DOI : https://doi.org/10.1016/j.bbamem 2008.10.006, **1788**, 149–168, (2009).
2. Klein, M.L. Shinoda, W. Large-Scale Molecular Dynamics Simulations of Self-Assembling Systems. *Science.* DOI: 10.1126/science.1157834, *321*, 798–800, (2008).
3. Voth, G.A. *Coarse-graining of Condensed Phase and Biomolecular Systems*; Taylor & Francis/CRC press, Chapter **11**, 157-170, (2009).
4. Marrink, S. J. De Vries,A. H. Mark, A. E. Coarse Grained Model for Semiquantitative Lipid Simulations. *J. Phys. Chem. B*, DOI: https://doi.org/10.1021/jp036508g, **108**, 750-760, (2004).
5. Zavadlav, J. Marrink, S.J. Praprotnik, SWINGER: a clustering algorithm for concurrent coupling of atomistic and supramolecular liquids. M. DOI: https://doi.org/10.1098/rsfs.2018.0075, *Interface Focus*, **9**, 20180075 (2019).
6. Lee, H. Pastor, R.W. Coarse-grained model for PEGylated lipids: effect of PEGylation on the size and shape of self-assembled structures. *J. Phys. Chem. B,* DOI: https://doi.org/10.1021/jp2020148, **115**, 7830-7837, (2011).
7. Liu, Y. Barnoud, J. Marrink, S.J. Gangliosides Destabilize Lipid Phase Separation in Multicomponent Membranes. *Membranes Biophys. J.* DOI: https://doi.org/10.1016/j.bpj.2019.08.037, **117**, 1215-1223,(2019).

8. L. Monticelli, S.K.Kandasamy, X. Periole, R.G. Larson, D.P.Tieleman, S.J.Marrink, The MARTINI Coarse-Grained Force Field: Extension to Proteins, *J. Chem. Theor. Comput.* DOI: https://doi.org/10.1021/ct700324x, **4,** 819-834 (2008).

9. S.Koch, M. Exterkate, C.A. López, M. Patro, S.J. Marrink, A.J.M. Driessen, Two distinct anionic phospholipid-dependent events involved in SecA-mediated protein translocation. *BBA-Biomembr*. DOI: https://doi.org/10.1016/j.bbamem.2019.183035 **1861(11)**, 183035 (2019).

10. Corradi, V. Mendez-Villuendas, E. Ingólfsson, H.I. Gu, R.X. Siuda, I. Melo, M.N. Moussatova, A.DeGagné, L.J. .Sejdiu, B.I. Singh, G.T. Wassenaar, A.Magnero, K.D. Marrink,S.J. Tieleman, D.P. Lipid–Protein Interactions Are Unique Fingerprints for Membrane Proteins. DOI: http://pubs.acs.org/doi/abs/10.1021/acscentsci.8b00143 *ACS Central Science,* **4(6)** 709–717 (2018).

11. Lee, H. De Vries, A H. Marrink, S.J. Pastor, R.W. A coarse-grained model for polyethylene oxide and polyethylene glycol: conformation and hydrodynamics. *J. Phys. Chem. B*, DOI: https://doi.org/10.1021/jp9058966, **113(40)**: 13186-13194 (2009).

12. Xue,M. Cheng, L. Faustino, I. Guo, W. Marrink, S.J. Molecular Mechanism of Lipid Nanodisk Formation by Styrene-Maleic Acid Copolymers. *Biophys. J.* DOI: https://doi.org/10.1016/j.bpj.2018.06.018, **115(3):** 494-502, (2018).

13. Milani, A. Casalegno, M. Castiglioni,C. Raos, G. Coarse-Grained Simulations of Model Polymer Nanofibres. *Macromol Theor. Simul.* DOI: https://doi.org/10.1002/mats.201100010, **20(5):** 305-319, (2011) .

14. A.López, C. Rzepiela, A. J. De Vries, A. H. Dijkhuizen, L. Hünenberger, P.H. Marrink, S.J. Martini Coarse-Grained Force Field: Extension to Carbohydrates. *J. Chem. Theor. Comput.* DOI: https://doi.org/10.1021/ct900313w, **5(12):** 3195-3210, (2009).

15. Wohlert, J. Berglund, L.A. A Coarse-Grained Model for Molecular Dynamics Simulations of Native Cellulose. *J. Chem. Theor. Comput.* DOI: https://doi.org/10.1021/ct100489z, **7(3):** 753-760, (2011)..

16. Frederix, P.W.J.M.Patmanidis, I. Marrink, S.J. Molecular simulations of self-assembling bio-inspired supramolecular systems and their connection to experiments. *Chem. Soc. Rev.* DOI: 10.1039/C8CS00040A, **47(10):** 3470-3489, (2018).

17. Kondela, T. Gallová, J. Hauß, T. Barnoud, J. Marrink, S. J. Kučerka, N. Alcohol Interactions with Lipid Bilayers. *Molecules,* DOI: https://doi.org/10.3390/molecules22122078, **22(12):** 2078 (2017).

5

18. Bruininks, B.M.H. Souza, P.C.T. Marrink, S. J. A Practical View of the Martini Force Field. *Biomolecular Simulations,* DOI: http://doi.org/10.1007/978-1-4939-9608-7_5, Humana, New York, NY, 105-127 (2019).

19. Sangwai, A.V. Sureshkumar, R. Coarse-grained molecular dynamics simulations of the sphere to rod transition in surfactant micelles. *Langmuir,* **27(11):** 6628-6638, (2011).

20. Burov, S.V. Obrezkov, N.P. Vanin, A.A M.Piotrovskaya, E. Molecular dynamic simulation of micellar solutions: A coarse-grain model. *Colloid J.* DOI: https://doi.org/10.1134/S1061933X08010018, *70(1):* 1-5, (2008).

21. Wu, R. Deng, M. Kong, B. Yang, X.Coarse-Grained Molecular Dynamics Simulation of Ammonium Surfactant Self-Assemblies: Micelles and Vesicles. *J. Phys. Chem. B* , DOI: https://doi.org/10.1021/jp906055d, **113(45):** 15010-15016, (2009).

22. Pérez-Sánchez, G. Gomes, J. R. Jorge, M. Modeling Self-Assembly of Silica/Surfactant Mesostructures in the Templated Synthesis of Nanoporous Solids. *Langmuir,* DOI: https://doi.org/10.1021/la3046274, **29(7)**, 2387-2396, (2013).

23. Jalili, S. Akhavan, M. A coarse-grained molecular dynamics simulation of a sodium dodecyl sulfate micelle in aqueous solution. *Colloids Surfaces A*, DOI: https://doi.org/10.1016/j.colsurfa.2009.10.007, **352(1-3),** 99-102 (2009).

24. Kraft, J.F. Vestergaard, M. Schiøtt, B. Thøgersen, L. Modeling the Self-Assembly and Stability of DHPC Micelles Using Atomic Resolution and Coarse Grained MD Simulations. *J. Chem. Theor. Comput.* DOI: https://doi.org/10.1021/ct200921u, **8(5),** 1556-1569, (2012).

25. Velinova, M. Sengupta, D. Tadjer, A.V. Marrink, S. J. Sphere-to-Rod Transitions of Nonionic Surfactant Micelles in Aqueous Solution Modeled by Molecular Dynamics Simulations. *Langmuir,* DOI:https://doi.org/10.1021/la203055t, **27(23),** 14071-14077, (2011).

26. A.Sanders, S. Panagiotopoulos, A.Z. Micellization behavior of coarse grained surfactant models, *J. Chem. Phys.* DOI: https://doi.org/10.1063/1.3358354, **132**, 114902 (2010).

27. Marrink, S.J. Tieleman, D.P. Perspective on the Martini model. *Chem. Soc. Rev.* DOI: http://doi.org/10.1039/C3CS60093A, **42(16)**, 6801-6822, (2013).

28. Tong, S.J. Cao, F.L. Xin, Sun, L.H. Formation of microemulsion particles with surfactant—A coarse-grained molecular dynamics simulation study. *Scientia Sinica Chimica,* DOI: https://doi.org/10.1360/032013-169, **(43)**, 1557-1565, (2013).

29. Wang, H. Zhang, H. Liu, C. Yuan, S. Coarse-grained molecular dynamics simulation of self-assembly of polyacrylamide and sodium dodecylsulfate in aqueous solution *J. Colloid Inter.* DOI: https://doi.org/10.1016/j.jcis.2012.07.026, **386(1),** 205-211, (2012).

30. Abraham, M.J. Murtola, T. Schulz, R. Páll, C.Smith, S.J. Hess, B. Lindahl, E. GROMACS: High performance molecular simulations through multi-level parallelism from laptops to supercomputers. *SoftwareX*, DOI: https://doi.org/10.1016/j.softx.2015.06.001, **1**, 19-25, (2015).

31. Berendsen, H.J.C. Grigera, J.R. Straatsma, T.P. The missing term in effective pair potentials. *J. Phys. Chem.* DOI:https://doi.org/10.1021/j100308a038, **91(24)**, 6269-6271 (1987).

32. Jorgensen, W.L. Maxwell, D.S. Tirado-Rives,J. Development and Testing of the OPLS All-Atom Force Field on Conformational Energetics and Properties of Organic Liquids. *J. Am.Chem. Soc.* DOI: https://doi.org/10.1021/ja9621760, **118(45),** 11225-11236, (1996).

33. Molecular Dynamics in Physiological Solutions: Force Fields, Alkali Metal Ions, and Ionic Strength. C.Zhang, S.Raugei, B.Eisenberg, P.Carloni, *J Chem Theory Comput.* DOI:https://doi.org/10.1021/ct9006579, **6(7)**, 2167-2175, (2010).

34. Jia, X. Yu, S. Ma, Y. Li,X. Xu,W. Liu, J. Model of cylindrical micelles with different endcaps. *J. Disper. Sci.Technol*. DOI: https://doi.org/10.1080/01932691.2016.1185016, **38(5)**, 621-625, (2017).

35. Chen, J. Long, P. Li, H. Hao, J. Investigations into the Bending Constant and Edge Energy of Bilayers of Salt-Free Catanionic Vesicles. *Langmuir,* DOI: https://doi.org/10.1021/la2048773, 28(14), 5927-5933, (2012) .

36. Johnson, J.K. Zollweg, J.A. Gubbins, K.E. The Lennard-Jones equation of state revisited. *Mol. Phys.* DOI: https://doi.org/10.1080/00268979300100411,**78(3)**, 591-618 (1993) .

Acknowledgements

This work was supported by Major Scientific and Technological Innovation Project (2019JZZY020211) and the National Key Research and Development Program of China (2017YFF0209904).

Author contributions statement

Xiang-feng Jia and Jing-fei Chen conceived the Methods, and conducted the discussions and the conclusions, Xiang-feng Jia, Jingfei Chen and Hui-xue Ren analysed the results. All authors reviewed the manuscript.

,

Figures

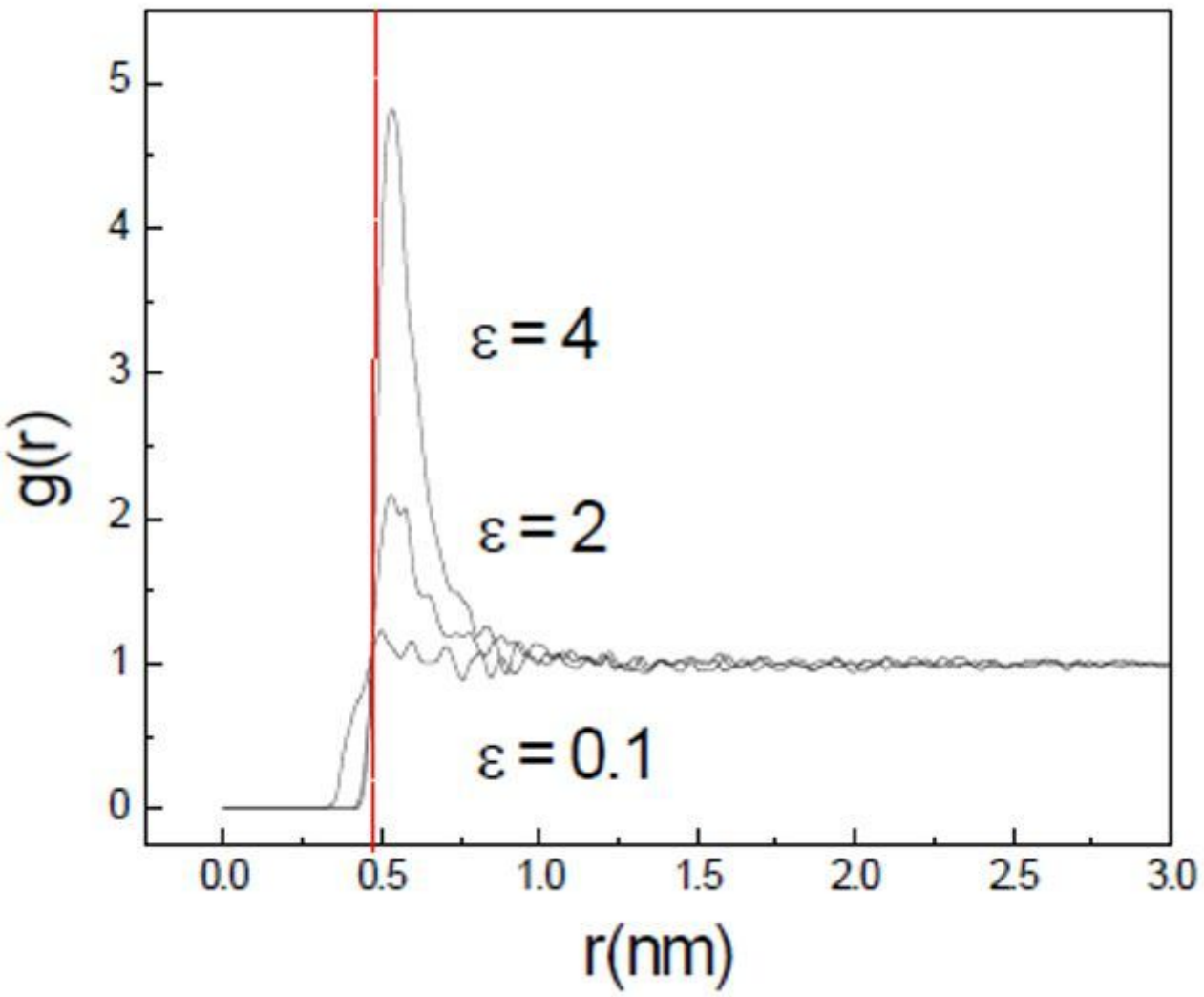

Figure 1

In the single-component Van der Waals systems, the radial distribution function (RDF) of the particles with the same (0.47nm) but different (0.1, 2, 4 KJ/mol). The value are indicated by the dash line.

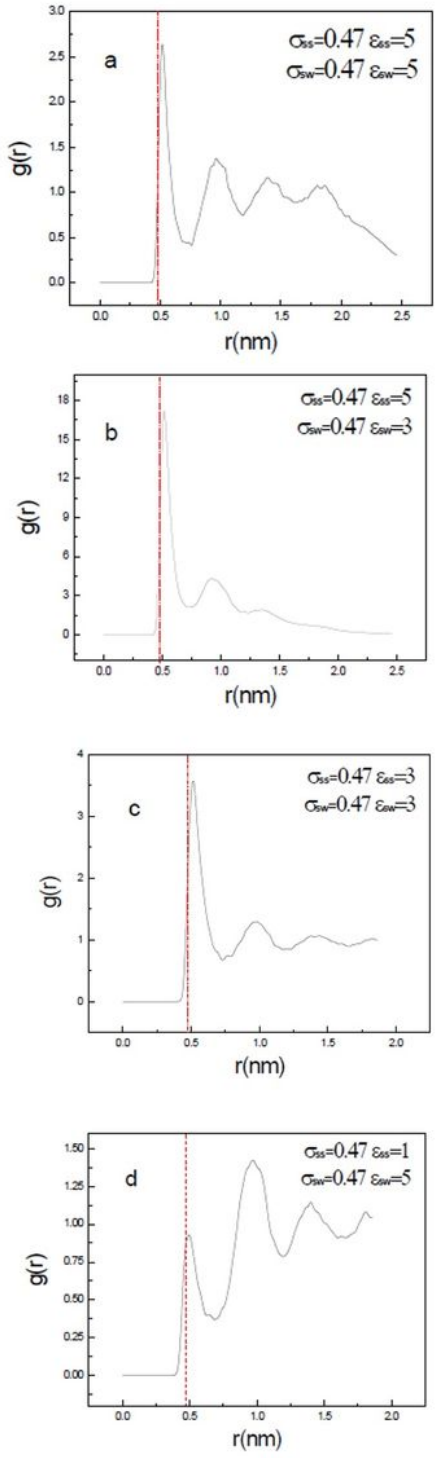

Figure 2

RDF of particles with different polarity and solubility in the same solvent, gs-s(r). σss(0.47nm) are indicated by dash lines.

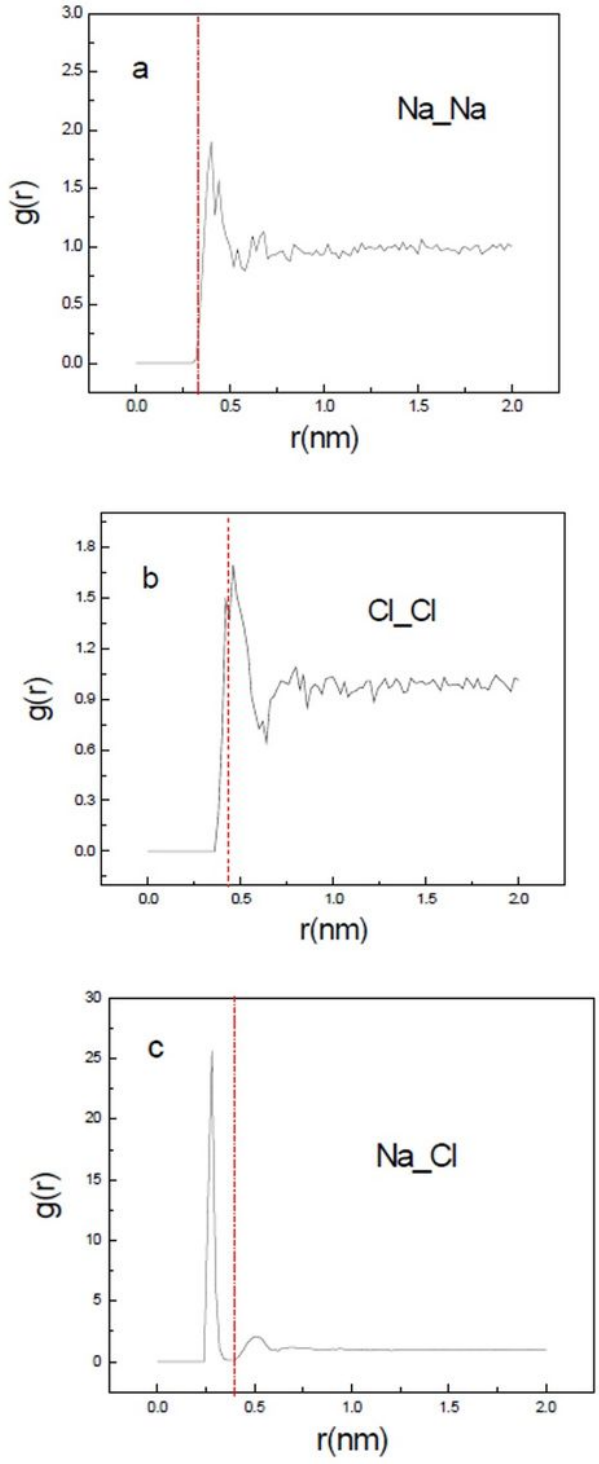

Figure 3

RDF between the charged particles in the NaCl solution, the σ values between the particles was indicated by dash lines.

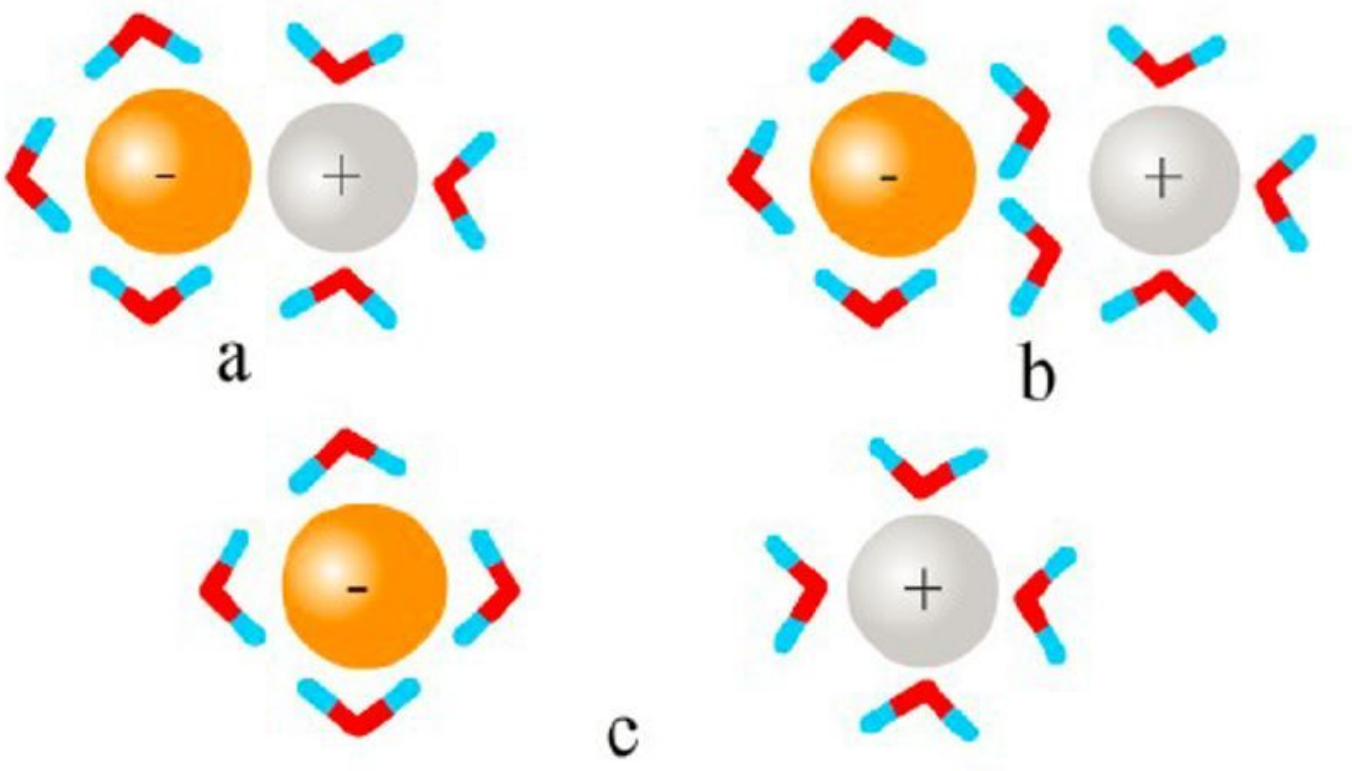

Figure 4

Different hydration states of Na+ and Cl- in NaCl solution

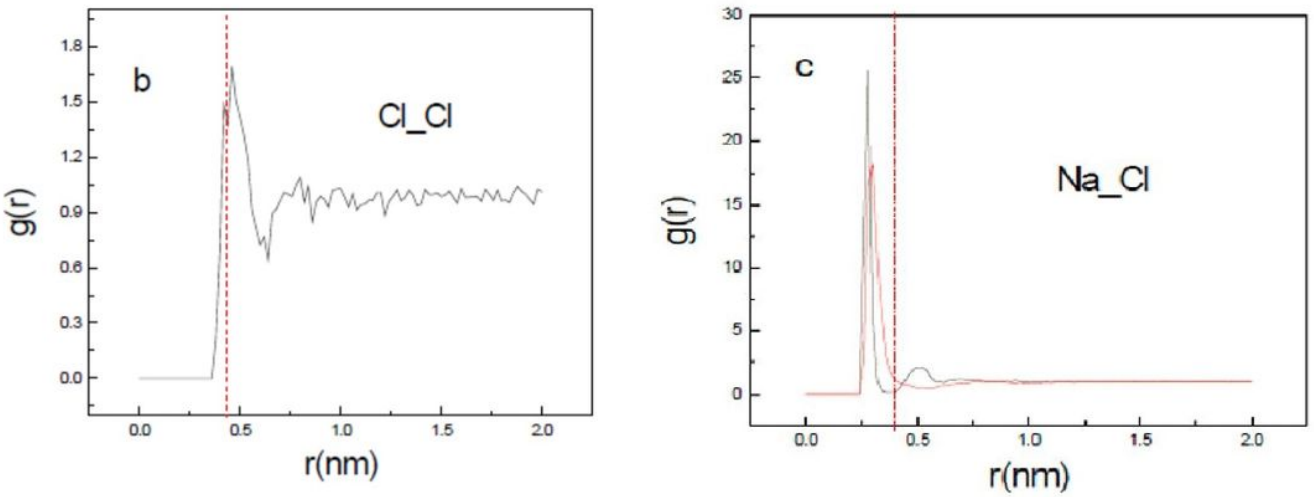

Figure 5

The RDF of ions in NaCl coarse grained system

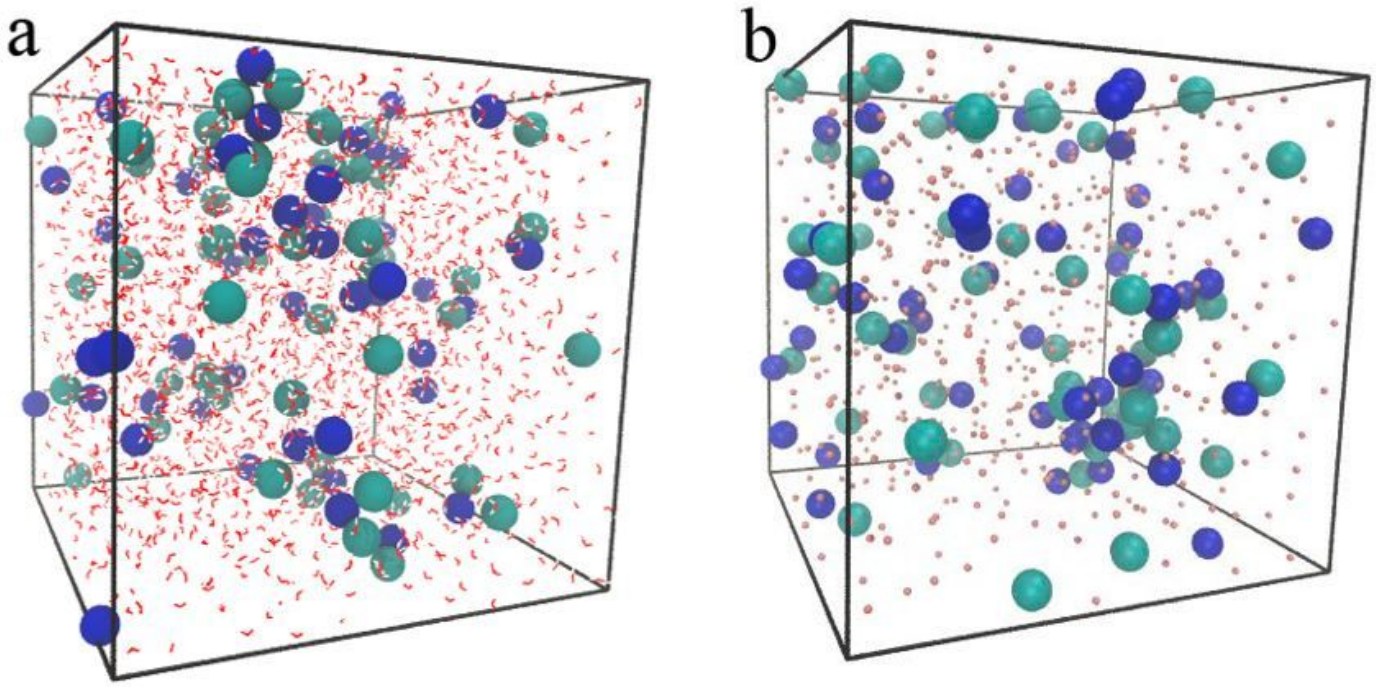

Figure 6

NaCl solution was simulated using OPLS-aa (a) and CG (b) force filed

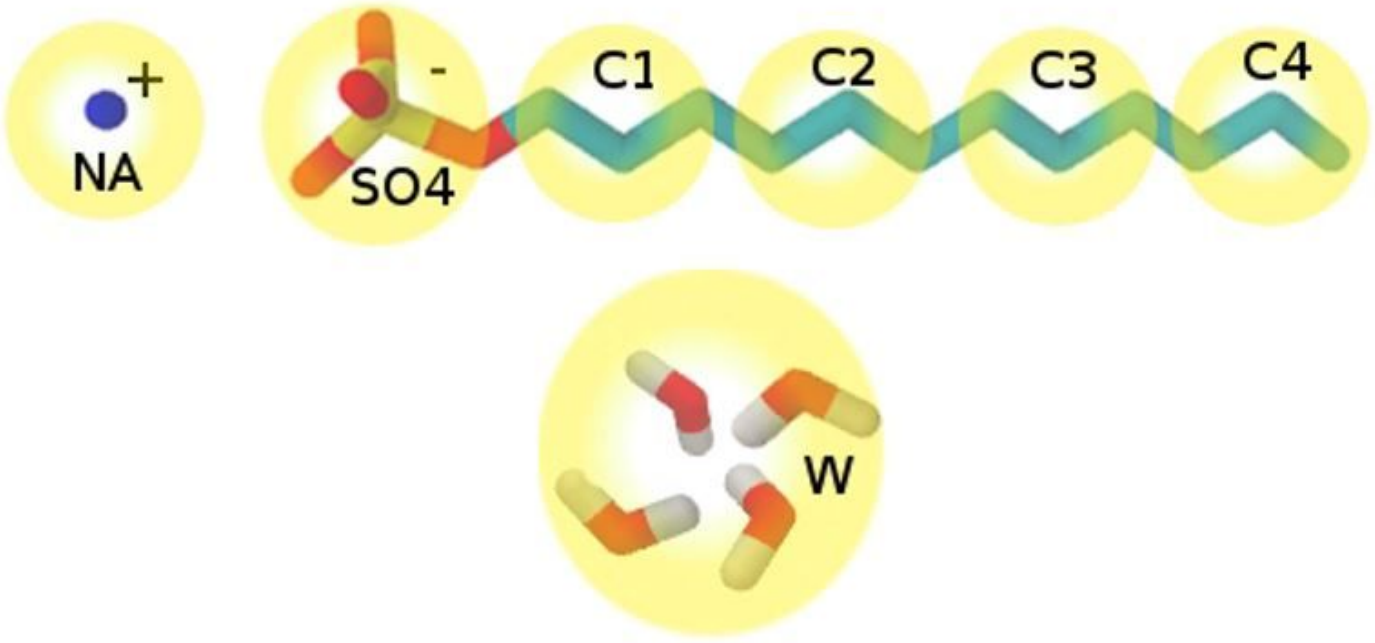

Figure 7

Coarse grained model of SDS

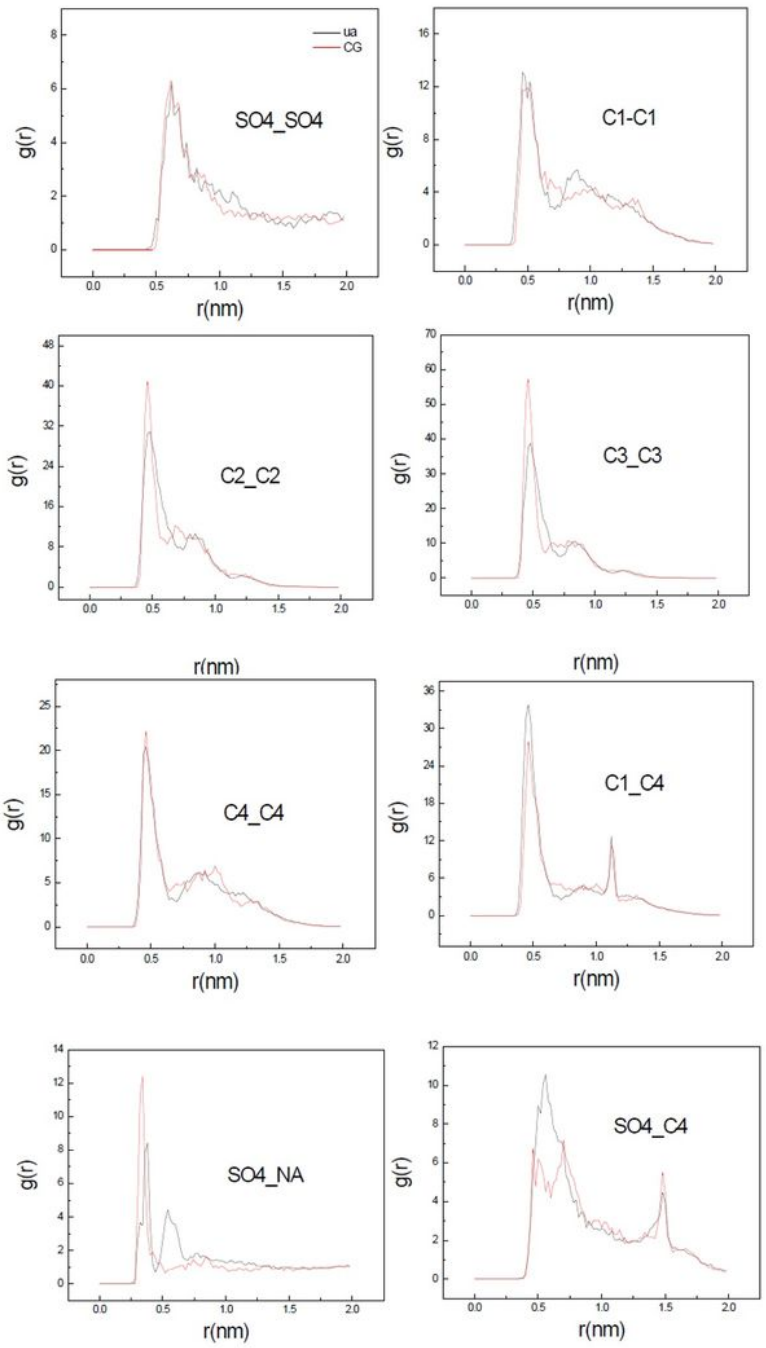

Figure 8

RDF of different units of SDS in unitedatomic (ua:—) and Coarse-grained (CG:—) simulation

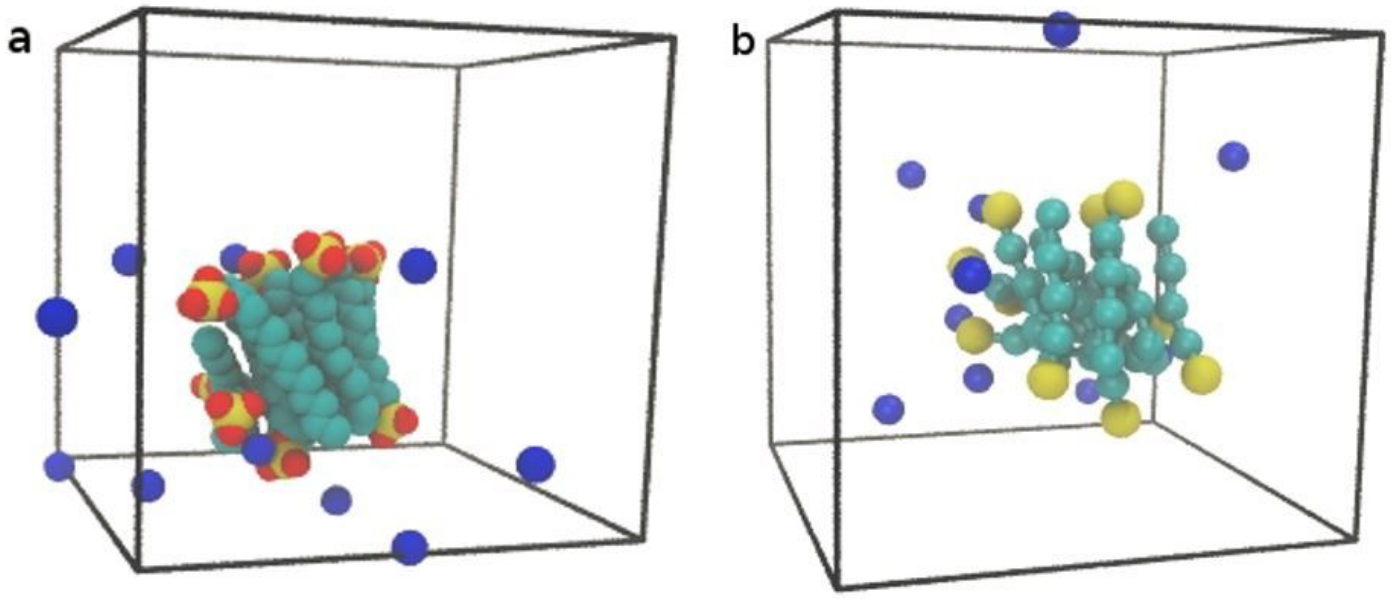

Figure 9

The snapshots of SDS micelles in atomistic (a) and coarse grained (b) simulation

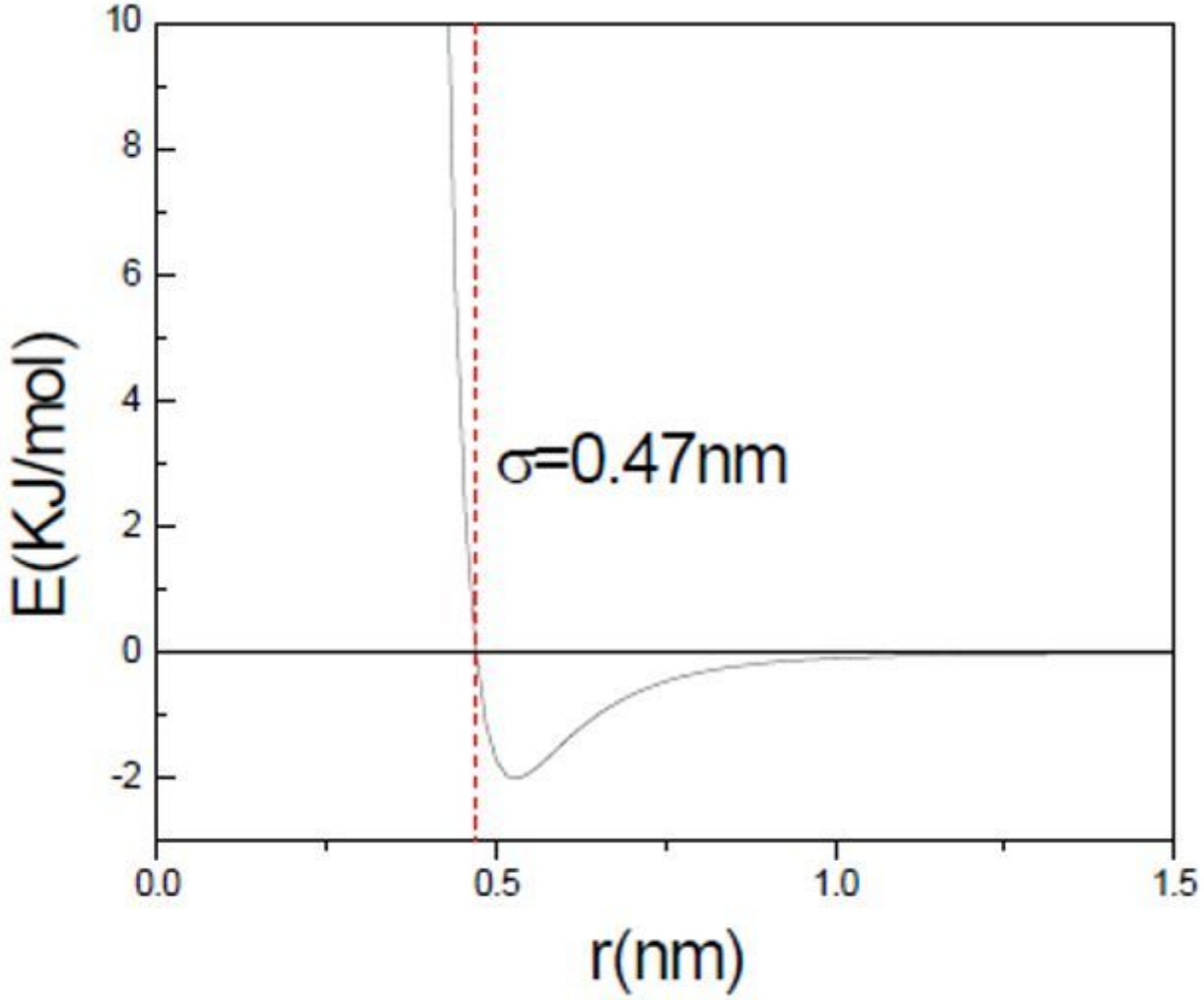

Figure 10

Lennard-Jones interaction (12-6)